National Conference with International Participation
ENGINEERING MECHANICS 2006
Svratka, Czech Republic, May 15 – 18, 2006
paper no. 281

MODELLING AND DYNAMICAL ANALYSIS OF GEAR DRIVES VIBRATION CONSIDERING THE INFLUENCE OF NONLINEAR COUPLINGS

M. Byrtus, V. Zeman[1]

Summary: *Gear drives and gearboxes are parts of many mechanical devices and simultaneously represent main excitation sources. The aim of this contribution is to take into account the influence of nonlinear couplings in the gear drives and create a general mathematical model for an arbitrary gearbox using the modal synthesis method with DOF number reduction. The stress is laid on nonlinear modelling of gear and bearing couplings and their influence on the dynamical system response to the internal excitation. The bearing model respects real number of rolling bodies and real roller nonlinear contact forces acting between journals and the outer housing in dependance on their deflection. The nonlinear model of gear meshing makes possible to respect in consequence of low static load and internal excitation generated in gear meshing the the gear mesh interruption. As a result of nonlinear couplings, vibrations are accompanied by impact motions, bifurcation of solution and chaotic motions. The presented approach to the nonlinear vibration analysis of large multibody gear drives is applied to a simple test-gearbox.*

1. Introduction

Large rotating systems, especially gear drives and gearboxes occur as parts of many mechanical devices on one hand. But they are representans of main excitation sources on the other hand. Their vibration analyses are commonly performed with the assumption of the small deformations and linearized coupling forces. But this assumption is not correct for certain operational states when the influence of coupling nonlinearities is dominant. Therefore the nonlinear models of gear and bearing couplings are developed and the influence of coupling nonlinearities is investigated.

In last years the subject of large rotating systems modelling has been studied in our department. The result of this effort is a creation of modal synthesis method allowing to model systems with complicated structures. The advantage of this method is separate modelling of subsystems

[1] Ing. Miroslav Byrtus, Prof. Ing. Vladimír Zeman, DrSc., Department of Mechanics, Faculty of Applied Sciences, University of West Bohemia in Pilsen, Univerzitní 8, 306 14 Plzeň, tel. +420 377 63 23 15, e-mail: byrtus@kme.zcu.cz

using different modelling tools and separate modelling of discrete couplings. Subsequently the noise radiation analysis can be performed, as Hajžman and Byrtus (2006) have shown.

A general mathematical model of a large rotating system including the flexible stator is created and solution of nonlinear dynamical response is shown. Gear kinematic transmission errors are supposed to be the main source of high-frequency vibrations. A simple test-gearbox is used for numerical experiments to test the presented modelling methodology.

2. Modelling of large rotating systems

To model large rotating system the modal synthesis method is used. This method is based on suitable system decomposition into subsystems and on separate modelling of couplings among subsystems. In our case, the gearbox can be generally decomposed into S subsystems. The first $S-1$ subsystems which consist of shafts with gears rotating with angular velocity ω_s are described with following system of ordinary differential equation in matrix form as Zeman and Hlaváč (1995) showed

$$\boldsymbol{M}_s\ddot{\boldsymbol{q}}_s(t) + (\boldsymbol{B}_s + \omega_s\boldsymbol{G}_s)\dot{\boldsymbol{q}}_s(t) + \boldsymbol{K}_s\boldsymbol{q}_s(t) = \boldsymbol{f}_s^E(t) + \boldsymbol{f}_s^G + \boldsymbol{f}_s^B,\ s = 1,\, 2,\, \ldots,\, S-1, \quad (1)$$

where $\boldsymbol{M}_s$, $\boldsymbol{B}_s$ and $\boldsymbol{K}_s$ are symmetrical mass, damping and stiffness matrices of the uncoupled subsystems of order n_s and $\boldsymbol{G}_s$ is skew symmetrical matrix of the gyroscopic effects of the same order. These matrices are usually created by means of finite element method combined with discrete parameters representing masses of rigid gear discs. External forced excitation is described by vector $\boldsymbol{f}_s^E(t)$. Vector $\boldsymbol{f}_s^G$ represents the forces in spur helical gear couplings and vector $\boldsymbol{f}_s^B$ expresses the coupling forces in rolling-element bearings. All force effects described in vectors above are acting on the subsystem s. The mathematical model of the housing is expressed in a similar way

$$\boldsymbol{M}_S\ddot{\boldsymbol{q}}_S(t) + \boldsymbol{B}_S\dot{\boldsymbol{q}}_S(t) + \boldsymbol{K}_S\boldsymbol{q}_S(t) = \boldsymbol{f}_S^E(t) + \boldsymbol{f}_S^B. \quad (2)$$

Mass, damping and stiffness matrices $\boldsymbol{M}_S$, $\boldsymbol{B}_S$, $\boldsymbol{K}_S$ of order n_S are created after discretization by finite element method. Vector $\boldsymbol{f}_S^E(t)$ is a possible external excitation and force effect of bearing couplings is expressed by vector $\boldsymbol{f}_S^B$.

The bearing model, used in our approach to gearbox modelling, respects real number of rolling elements uniform distributed between the inner and outer race (see fig. 1). Let us suppose that the rolling-element j of the bearing i touches the outer race at the contact point $H_{i,j}$. The force $F_{i,j}$ trasmitted at this point depends nonlinearly on the rolling-element deflection $\Delta_{i,j}$ according the Hertz's contact theory in this way

$$F_{i,j} = \left(\frac{\Delta_{i,j}}{C}\right)^n H(\Delta_{i,j}), \quad F_{i,j}^{ax} = \left(\frac{\Delta_{i,j}^{ax}}{C}\right)^n H(\Delta_{i,j}^{ax}). \quad (3)$$

The designation ax belongs to axial deflections of rolling-elements and corresponding axial forces that moreover arise in the radi-axial rolling bearings. The deflections arise from the deformation of the of the rolling elements and the races at the contact point. Parameters n and C depend on rolling-elements geometry, elastic modulus and Poission's ratio of the bearing components, as mentioned in Krämer (1993). Heaviside function H corrects the contact forces when the deflections are negative which means that the rolling elements are unloaded.

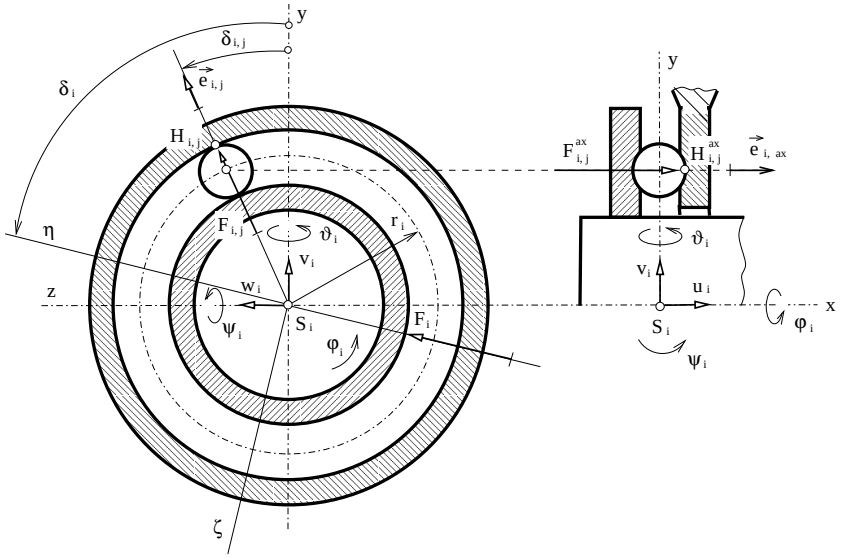

Figure 1: Scheme of a bearing coupling

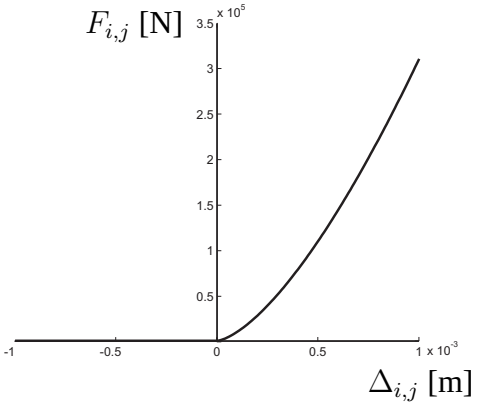

Figure 2: The ball-element bearing force characteristic

The calculation of the deflections $\Delta_{i,j}$ and $\Delta_{i,j}^{ax}$ supposing the rigid inner and flexible outer race, is in detail described in Byrtus and Zeman (2005). Fig. 2 shows the dependance of force transmitted by a rolling element on its deflection.

Then the vector $\boldsymbol{f}_s^B$ in equation (1) (model of rotating parts) can be expressed in following form

$$\boldsymbol{f}_s^B = -\sum_i \sum_j (\tilde{\boldsymbol{t}}_{i,j} F_{i,j}(\boldsymbol{q}_s) + \tilde{\boldsymbol{t}}_{i,j}^{ax} F_{i,j}^{ax}(\boldsymbol{q}_s)),\ s = 1, \ldots, S-1, \tag{4}$$

where vectors $\tilde{\boldsymbol{t}}_{i,j}$, $\tilde{\boldsymbol{t}}_{i,j}^{ax}$ describe the bearing geometry. Among bearing indices i belong only these which correspond to bearings coupled with the subsystem s. Similarly, the vector $\boldsymbol{f}_S^B$ in equation (2) (model of a stator – housing) can be expressed in following form

$$\boldsymbol{f}_S^B = \sum_i \sum_j (\tilde{\boldsymbol{e}}_{i,j} F_{i,j}(\boldsymbol{q}_S) + \tilde{\boldsymbol{e}}_{i,j}^{ax} F_{i,j}^{ax}(\boldsymbol{q}_S)), \tag{5}$$

where vectors $\tilde{\boldsymbol{e}}_{i,j}$, $\tilde{\boldsymbol{e}}_{i,j}^{ax}$ describe the geometry of contact points at the stator. Bearing indices i are governed by the same conditions as above.

In the general coordinate space

$$\boldsymbol{q}(t) = [\, \boldsymbol{q}_1^T(t),\ \boldsymbol{q}_2^T(t),\ \ldots\ ,\ \boldsymbol{q}_S^T(t)\,]^T \in \mathbb{R}^n, \quad n = \sum_{s=1}^{S} n_s \tag{6}$$

of the whole system the bearing model is described by the global coupling vector in the form

$$\boldsymbol{f}^B = \begin{bmatrix} \boldsymbol{f}_1^B \\ \boldsymbol{f}_2^B \\ \vdots \\ \boldsymbol{f}_S^B \end{bmatrix} = \sum_i \sum_j (\boldsymbol{c}_{i,j} F_{i,j}(\boldsymbol{q}) + \boldsymbol{c}_{i,j}^{ax} F_{i,j}^{ax}(\boldsymbol{q})). \tag{7}$$

Vectors $\boldsymbol{c}_{i,j}$ and $\boldsymbol{c}_{i,j}^{ax}$ describe global geometrical properties of each bearing contact point j in bearing i and have this structure

$$\boldsymbol{c}_{i,j} = \left[\, \cdots - \tilde{\boldsymbol{t}}_{i,j}^T \cdots \tilde{\boldsymbol{e}}_{i,j}^T \ \cdots \right]^T, \quad \boldsymbol{c}_{i,j}^{ax} = \left[\, \cdots - (\tilde{\boldsymbol{t}}_{i,j}^{ax})^T \cdots (\tilde{\boldsymbol{e}}_{i,j}^{ax})^T \ \cdots \right]^T. \tag{8}$$

To stabilize the numerical simulation of the nonlinear model it is efficient to separate the linear part of nonlinear bearing force characteristic. The linear part is described by stiffness and damping matrices in the general coordinate space (6) and the bearing force vector (7) can be then rewritten in following form

$$\boldsymbol{f}^B = -\boldsymbol{K}_B \boldsymbol{q}(t) - \boldsymbol{B}_B \dot{\boldsymbol{q}}(t) + \sum_i \sum_j (\boldsymbol{c}_{i,j} f_{i,j}(\boldsymbol{q}) + \boldsymbol{c}_{i,j}^{ax} f_{i,j}^{ax}(\boldsymbol{q})), \tag{9}$$

where $\boldsymbol{K}_B$ and $\boldsymbol{B}_B$ are global stiffness and damping bearing matrices. Their structure depends on the number of rolling elements and on the nodal points to which are they on the shafts fixed (for details see Zeman and Hajžman (2005)). The bearing damping matrix is supposed to be proportional to the stiffness matrix

$$\boldsymbol{B}_B = \beta_B \boldsymbol{K}_B \tag{10}$$

and functions $f_{i,j}$ have form

$$f_{i,j}(\boldsymbol{q}) = \left[\left(\frac{\Delta_{i,j}(\boldsymbol{q})}{C} \right)^n - k_{i,j} \Delta_{i,j}(\boldsymbol{q}) \right] H(\Delta_{i,j}(\boldsymbol{q})) - k_{i,j} \Delta_{i,j}(\boldsymbol{q}) H(-\Delta_{i,j}(\boldsymbol{q})). \tag{11}$$

In the same way can be expressed the function $f_{i,j}^{ax}(\boldsymbol{q})$. The parameters $k_{i,j}$ represent linearized rolling-elements stiffness that is calculated in dependence on an external static torsional loading of drive and driven shafts as is shown in Byrtus and Zeman (2005).

The force effect of the spur helical gear coupling z in (1) is expressed by vector

$$\boldsymbol{f}_s^G = \pm \sum_z \tilde{\boldsymbol{\delta}}_{z,i} F_z(t, d_z, \dot{d}_z), \tag{12}$$

where sign "-" (minus) corresponds to driving gear and sign "+" (plus) corresponds to driven gear. Vector $\tilde{\boldsymbol{\delta}}_{z,i} = [\ldots, \boldsymbol{\delta}_{z,i}^T, \ldots]^T$ is the n_s-dimensional extended vector of geometrical parameters of the gear that is fixed on the shaft at the nodal point i. The force F_z transmitted by gearing z can be approximately expressed in the form

$$F_z(t, d_z, \dot{d}_z) = k_z(t) d_z + b_z \dot{d}_z + f_z(t, d_z), \tag{13}$$

where $k_z(t)$ is time dependent meshing stiffness and b_z is coefficient of viscous damping of gearing on gear mesh line. Nonlinear function $f_z(t, d_z)$ of gearing deformation d_z corrects the linear elastic part $F_z^{(e)}$ of the force F_z in the phases of the mesh gear interruption. According to $F_z^{(e)}$ shown in fig. 3, this non-linear function is expressed in form

$$f_z(t, d_z) = -k_z(t) d_z H(-d_z) + k_z(t)(d_z + u_z) H(-d_z - u_z), \tag{14}$$

where u_z is tooth backlash and H is Heaviside function.

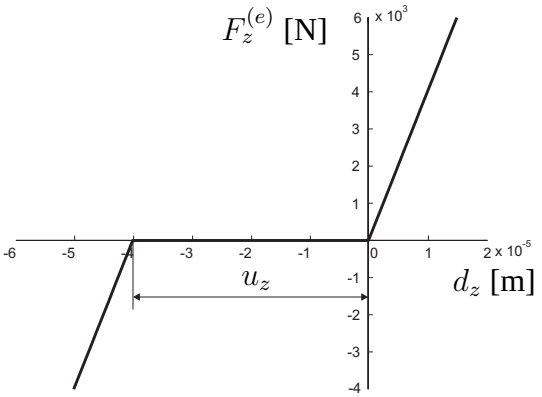

Figure 3: The elastic gearing force characteristic

Gearing deformation

$$d_z(t) = -\boldsymbol{\delta}_{z,i}^T \boldsymbol{q}_i(t) + \boldsymbol{\delta}_{z,j} \boldsymbol{q}_j(t) + \Delta_z(t), \tag{15}$$

of gears in mesh fixed on shafts at nodal points i and j expresses the relative motion of theoretical contact point of teeth on the gear mesh line. Vectors $\boldsymbol{q}_i(t)$ and $\boldsymbol{q}_j(t)$ describe displacements of nodal points i and j. The function $\Delta_z(t)$, defining kinematic transmission error of gearing z, can be expressed by Fourier series

$$\Delta_z(t) = \sum_{k=1}^{K} (\Delta_{z,k}^C \cos k\omega_z t + \Delta_{z,k}^S \sin k\omega_z t), \tag{16}$$

where meshing frequencies $\omega_z = \frac{\pi n}{30} p_z$ are functions of operation speed n [rpm] and $p_z = \frac{\omega_z}{\omega_0}$ is the speed ratio in relation of driving shaft of the gearbox.

Analogous to the bearing model, we can express the global gear coupling vector in general coordinate space (6) in following way

$$\boldsymbol{f}^G = \begin{bmatrix} \boldsymbol{f}_1^G \\ \boldsymbol{f}_2^G \\ \vdots \\ \boldsymbol{f}_{S-1}^G \\ \boldsymbol{0} \end{bmatrix} = \sum_{z=1}^{Z} \boldsymbol{c}_z F_z(t, \boldsymbol{q}, \dot{\boldsymbol{q}}) + \boldsymbol{f}_G(t), \tag{17}$$

where $\boldsymbol{f}_G(t)$ is vector of internal kinematic excitation generated in gear meshing that can be expressed in form

$$\boldsymbol{f}_G(t) = \sum_{z=1}^{Z} \left(k_z \Delta_z(t) + b_z \dot{\Delta}_z(t) \right) \boldsymbol{c}_z. \tag{18}$$

The global vector of geometrical parameters of the gearing z in general coordinate space (6) has following structure

$$\boldsymbol{c}_z = \left[\cdots \; -\boldsymbol{\delta}_{z,i}^T \; \cdots \; \boldsymbol{\delta}_{z,j}^T \; \cdots \middle| \; \mathbf{0}^T \right]^T . \tag{19}$$

For the same reason as above, it is efficient to separate up the linear part of nonlinear gearing force characteristic. Equation (17) can be then rewritten to this form

$$\boldsymbol{f}^G = -\boldsymbol{K}_G \boldsymbol{q}(t) - \boldsymbol{B}_G \dot{\boldsymbol{q}}(t) + \sum_{z=1}^{Z} \boldsymbol{c}_z F_z^N(t, \boldsymbol{q}) + \boldsymbol{f}_G(t). \tag{20}$$

$\boldsymbol{K}_G$ and $\boldsymbol{B}_G$ are stiffness and damping matrices of gear couplings, whose structure is in detail described in Zeman and Hajžman (2005) and the function F_z^N expresses the nonlinear part of the force transmitted by gearing z, i.e. $F_z^N(t, \boldsymbol{q}) = f_z(t, d_z)$.

It is advantageous to assemble condensed mathematical model of the system with reduced degrees of freedom (DOF) number, because mainly the housing subsystem could have too large DOF number and this can hinder from consecutive performing of various dynamical analyses and optimization. The modal transformations

$$\boldsymbol{q}_s(t) = {}^m\boldsymbol{V}_s \boldsymbol{x}_s(t), \qquad s = 1, 2, \ldots, S, \tag{21}$$

are introduced for this purpose. Matrices ${}^m\boldsymbol{V}_s \in \mathbb{R}^{n_s, m_s}$ are modal submatrices obtained from modal analysis of the mutually uncoupled, undamped and non-rotating subsystems, whereas m_s ($m_s \leq n_s$) is the number of the chosen master modes of vibration. The new configuration space of the dimension m is defined by vector

$$\boldsymbol{x}(t) = [\, \boldsymbol{x}_1^T(t), \, \boldsymbol{x}_2^T(t), \, \ldots \, , \, \boldsymbol{x}_S^T(t) \,]^T, \qquad m = \sum_{s=1}^{S} m_s. \tag{22}$$

The models (1) and (2) can be then rewritten using terms (17) and (9) in the global condensed form

$$\begin{aligned} \ddot{\boldsymbol{x}}(t) + \Big(\boldsymbol{B} + \omega_0 \boldsymbol{G} + \boldsymbol{V}^T (\boldsymbol{B}_B + \boldsymbol{B}_G) \boldsymbol{V} \Big) \dot{\boldsymbol{x}}(t) \; + \Big(\boldsymbol{\Lambda} + \boldsymbol{V}^T (\boldsymbol{K}_B + \boldsymbol{K}_G) \boldsymbol{V} \Big) \boldsymbol{x}(t) = \\ = \boldsymbol{V}^T \Big(\sum_i \sum_j (\boldsymbol{c}_{i,j} f_{i,j}(\boldsymbol{q}) + \boldsymbol{c}_{i,j}^{ax} f_{i,j}^{ax}(\boldsymbol{q})) + \sum_{z=1}^{Z} \boldsymbol{c}_z F_z^N(t, \boldsymbol{q}) + \boldsymbol{f}_G(t) + \boldsymbol{f}_E(t) \Big) , \end{aligned} \tag{23}$$

where $\boldsymbol{f}_E(t) = [\, (\boldsymbol{f}_1^E(t))^T, \, (\boldsymbol{f}_2^E(t))^T, \, \ldots \, , \, (\boldsymbol{f}_S^E(t))^T \,]^T$ is the global vector of external excitation,

$$\boldsymbol{B} = \operatorname{diag} \left({}^m\boldsymbol{V}_s^T \boldsymbol{B}_s {}^m\boldsymbol{V}_s \right), \quad \boldsymbol{G} = \operatorname{diag} \left(\frac{\omega_s}{\omega_0} {}^m\boldsymbol{V}_s^T \boldsymbol{G}_s {}^m\boldsymbol{V}_s \right), \quad \boldsymbol{V} = \operatorname{diag} \left({}^m\boldsymbol{V}_s \right) \tag{24}$$

are block diagonal matrices ($\omega_S = 0$ holds for the stator subsystem) and $\boldsymbol{\Lambda} = \operatorname{diag} \left({}^m\boldsymbol{\Lambda}_s \right)$ is diagonal matrix composed of spectral submatrices ${}^m\boldsymbol{\Lambda}_s \in \mathbb{R}^{m_s, m_s}$ of the subsystems.

3. Dynamical Analysis

The mathematical model of gear drives is strongly nonlinear due to the possibility of gear mesh interruption and in consequence of nonlinear bearing couplings respecting loss of contact in

some contact points in dependance on position of journal centre. To perform the dynamical analysis the condensed mathematical model (23) has to be transformed into the state space to use the direct-time integration method. The state space is described with vector of state variables in the form

$$\boldsymbol{u}(t) = [\,\dot{\boldsymbol{x}}_1^T(t),\ \dot{\boldsymbol{x}}_2^T(t),\ \ldots\ ,\ \dot{\boldsymbol{x}}_S^T(t),\ \boldsymbol{x}_1^T(t),\ \boldsymbol{x}_2^T(t),\ \ldots\ ,\ \boldsymbol{x}_S^T(t)\,]^T, \tag{25}$$

where the vectors $\boldsymbol{x}_s(t)$ were mentioned above. Then we can rewrite the mathematical model (23) into the state space in the general form

$$\boldsymbol{N}\dot{\boldsymbol{u}}(t) + \boldsymbol{P}\boldsymbol{u}(t) = \boldsymbol{F}(t, \boldsymbol{u}), \tag{26}$$

where

$$\boldsymbol{N} = \begin{bmatrix} \boldsymbol{0} & \boldsymbol{E} \\ \boldsymbol{E} & \boldsymbol{B}_{glob} \end{bmatrix}, \qquad \boldsymbol{P} = \begin{bmatrix} -\boldsymbol{E} & \boldsymbol{0} \\ \boldsymbol{0} & \boldsymbol{K}_{glob} \end{bmatrix}. \tag{27}$$

The initial conditions are

$$\boldsymbol{u}(0) = [\dot{\boldsymbol{x}}(0)^T\, \boldsymbol{x}(0)^T]^T. \tag{28}$$

The general form (26) can be rewritten using a system matrix denoted as $\boldsymbol{A}$ in a more suitable form

$$\dot{\boldsymbol{u}}(t) + \boldsymbol{A}\boldsymbol{u}(t) = \tilde{\boldsymbol{F}}(t, \boldsymbol{u}), \tag{29}$$

where $\boldsymbol{A} = \boldsymbol{N}^{-1}\boldsymbol{P}$ and $\tilde{\boldsymbol{F}}(t, \boldsymbol{u}) = \boldsymbol{N}^{-1}\boldsymbol{F}(t, \boldsymbol{u})$. The system matrix has following structure for the condensed model (23)

$$\boldsymbol{A} = \begin{bmatrix} \boldsymbol{B}_{\mathrm{glob}} & \boldsymbol{K}_{\mathrm{glob}} \\ -\boldsymbol{E} & \boldsymbol{0} \end{bmatrix}, \tag{30}$$

where $\boldsymbol{E}$ is a unit matrix and moreover it can be derived following relations

$$\begin{aligned} \boldsymbol{B}_{\mathrm{glob}} &= \boldsymbol{B} + \omega_0\boldsymbol{G} + \boldsymbol{V}^T\left(\boldsymbol{B}_B + \boldsymbol{B}_G\right)\boldsymbol{V}, \\ \boldsymbol{K}_{\mathrm{glob}} &= \boldsymbol{\Lambda} + \boldsymbol{V}^T\left(\boldsymbol{K}_B + \boldsymbol{K}_G\right)\boldsymbol{V} \end{aligned}$$

and

$$\tilde{\boldsymbol{F}}(t, \boldsymbol{u}) = \left[\boldsymbol{V}^T\left(\sum_{ij}(\boldsymbol{c}_{i,j}f_{i,j}(\boldsymbol{q}) + \boldsymbol{c}_{i,j}^{ax}f_{i,j}^{ax}(\boldsymbol{q})) + \sum_{z=1}^{Z}\boldsymbol{c}_z F_z^N(t, \boldsymbol{q}) + \boldsymbol{f}_G(t) + \boldsymbol{f}_E(t)\right)^T \quad \boldsymbol{0}^T\right]^T.$$

The aim of dynamical analysis is to investigate the behaviour of the system in dependence on chosen system parameters. Contrary of a linear system the nonlinear one can not be investigated using direct calculation of amplitudes of steady state periodical motion. There is a need to use some of the direct-time integration methods to gain the time response of the model (29) to arbitrary excitation. For this purpose, the time integration is started from initial state

$$\boldsymbol{x}(0) = (\boldsymbol{\Lambda} + \boldsymbol{V}^T(\boldsymbol{K}_B + \boldsymbol{K}_G)\boldsymbol{V})^{-1}\boldsymbol{V}^T\boldsymbol{f}_E(0)\,, \quad \dot{\boldsymbol{x}}(0) = \boldsymbol{0} \tag{31}$$

to minimize the startup transient motions. In general, the vector $\boldsymbol{f}_E(0)$ can describe an arbitrary external excitation at the start of numerical integration.

4. Nonlinear vibration of the test-gearbox

The presented methodology was verified using the simple test-gearbox (fig. 4). The gearbox was decomposed into two rotating shafts with gears ($s = 1,\ 2$) and into the housing ($s = 3$). Shafts were discretized using shaft finite elements and gears were modelled using their discrete parameters (mass and moments of inertia). The models of shaft subsystems were created and their modal analyses were performed in MATLAB code. The housing was modelled as 3D continuum using FEM in ANSYS system. The necessary housing modal values (eigenfrequencies and chosen eigenvectors) were exported from ANSYS to MATLAB. The condensed model of the whole system was assembled in MATLAB code on the basis of the presented methodology. MATLAB system was also used for the computation of the eigenvalues and dynamic response. The original nonreduced models of subsystems had together over 15 000 DOF and the first level of the model reduction had 580 DOF ($m_1 = m_2 = 90$, $m_3 = 400$). The final number of DOF was still reduced because the direct-time integration method, used here for dynamical analysis, is very time demanding. Thus, there is a need to find a sufficient DOF number to decrease computational time on one hand and to keep a sufficient results accuracy on other hand. The shaft

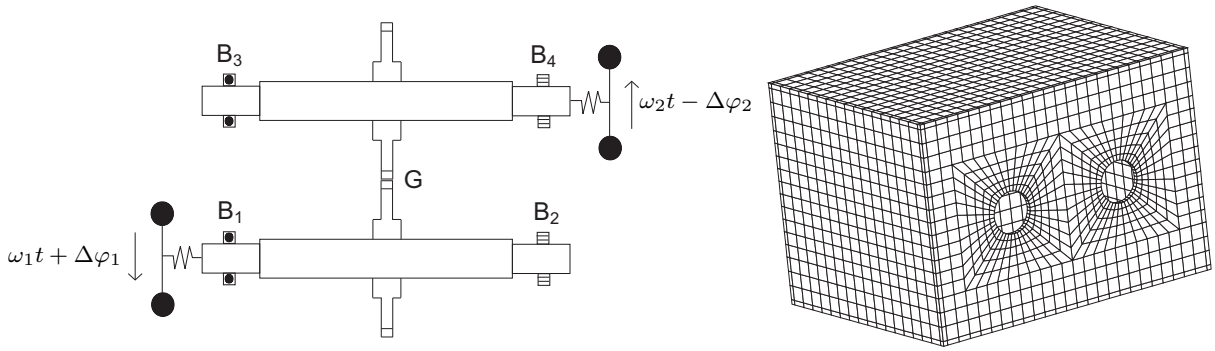

Figure 4: Scheme of the test-gearbox

system is included by means of flexible torsional couplings into a drive system. It is supposed constant angular speeds of the driving and driven parts of the system. Static external loading was defined by initial static torsional preloading $\Delta\varphi_1 = \Delta\varphi_2 = \Delta\varphi$ on both sides of the drive system (see fig. 4).

The approach to bearings modelling considers twenty rolling-elements for each bearing. The linearized parts of rolling elements stiffnesses in (11) are calculated from the non-linear system of algebraic equations which depend on static torsional loading $\Delta\varphi$ and are derived in Zeman and Hajžman (2005).

The system vibrations caused by internal kinematic excitation in gearing are investigated using the condensed model in dependence on static torsional preloading and on rotating speed of drive shaft using the direct-time integration method. The dynamical analysis was performed in dependence on operational revolutions n [rpm]. Kinematic transmission error in gear coupling ($z = 1$) was approximated by Fourier series with three harmonic components

$$\Delta^S_{1,1} = 5 \cdot 10^{-6}\,\mathrm{m}\,, \quad \Delta^S_{1,2} = \frac{\Delta^S_{1,1}}{2}\,, \quad \Delta^S_{1,3} = \frac{\Delta^S_{1,1}}{3}\,, \quad \Delta^C_{1,1} = \Delta^C_{1,2} = \Delta^C_{1,3} = 0\,.$$

We are concerned with the qualitative analysis of the test-gearbox vibrations. The aim is to investigate the influence of gear mesh interruption and contact loss of the rolling-elements

on the behaviour of the whole system. In fig. 5 and 6 the bifurcation diagrams of gearing deformation for a chosen revolution range of the system are shown. All results were gained for statical torsional preloading $\Delta\varphi = 0.06$ rad. In the diagram a line corresponding to zero gearing deformation is plotted. Each dot plotted under this line corresponds to gear mesh interruption. Red dots are maximal values of gearing deformation per one period of motion and the blue ones are minimal values, respectively. In the operational area there exist periodical solutions that may bifurcate to other periodical solutions with different number of maxima and with different number of impacts per one period of motion, or they may overcome to regions with chaotic motions. These regions of motions and changes among the regions are very interesting from the theoretical and practical point of view.

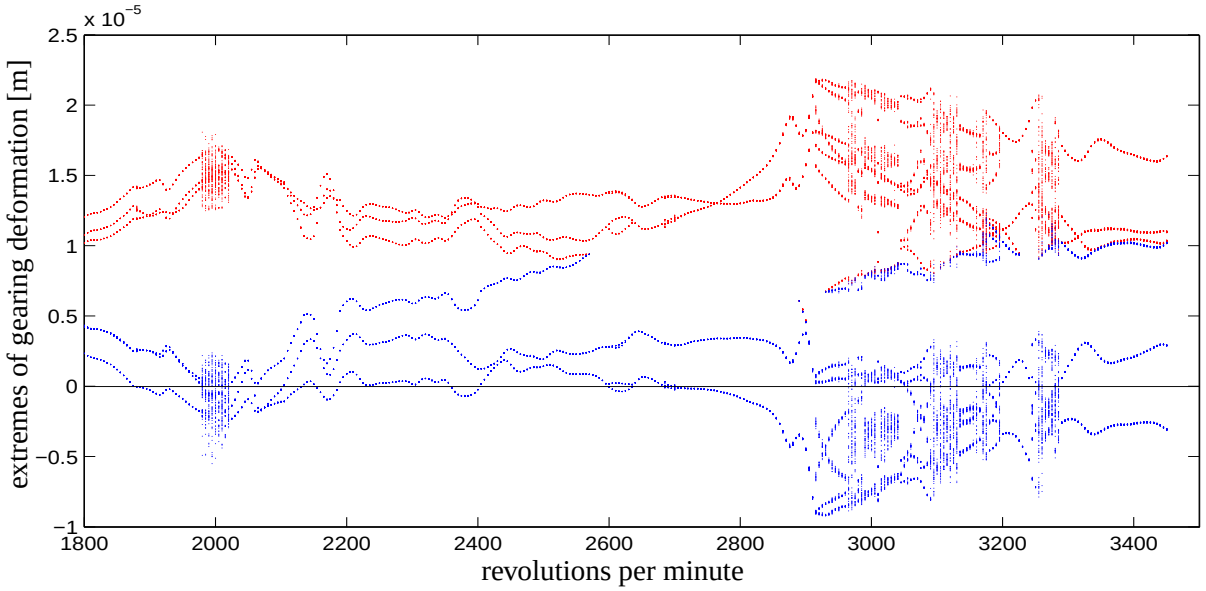

Figure 5: Bifurcation diagram. Dependence of extremes of gearing deformation on shaft's revolution for linearized bearing couplings

In fig. 5 and 6 we have a comparison of the influence of nonlinear couplings on gear mesh deformation. The first one shows the dependance of gearing deformation on shaft revolutions supposing the linearized bearing couplings without contact loss of rolling-elements.. The second one shows the same quantity but for nonlinear bearing couplings. The gear mesh behaviour seems to be very similar, but in case of nonlinear bearing the chaotic motion arise in such points, in which the simple bifurcation was for linearized bearing couplings.

In fig. 7 – 9 maxima and minima of chosen rolling-elements deformation are plotted. According the extreme deformation values we can specify whether the the rolling-element is loaded, or some impact motions among shaft, housing and rolling-element arise (transversal radial direction), or the rolling-element is unloaded, which is signified by negative deformation value (opposite the fully loaded element).

In fig. 10 phase trajectories of gearing deformation for three different states that are defined by $n = 2300$ rpm, $n = 2800$ rpm and $n = 3260$ rpm, respectively are plotted. The first state is characterized by motion with three maxima and minima per one period and no gear mesh interruption, the second one with two maxima and minima per one period and with one gear mesh interruption per the period of motion and the third one is chaotic with random gear mesh

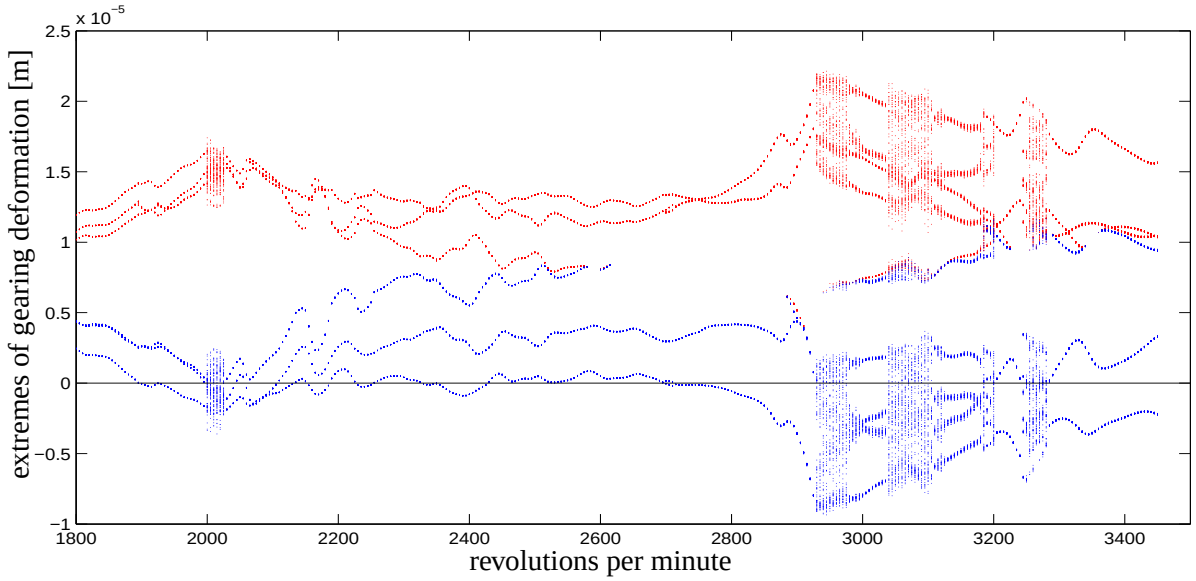

Figure 6: Bifurcation diagram. Dependence of extremes of gearing deformation on shaft's revolution for nonlinear bearing couplings

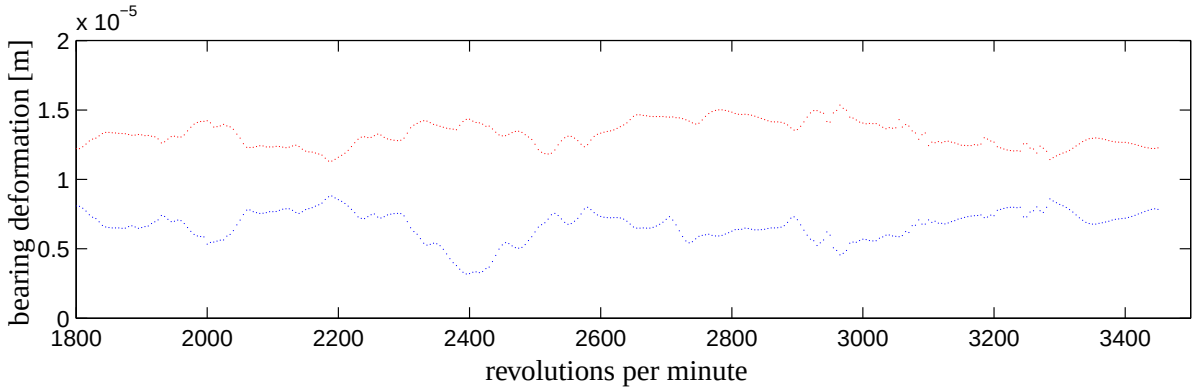

Figure 7: Dependence of extremes of roller-element bearing deformation on shaft's revolution for $\delta_{1,j} = \delta_1$ (main radial direction)

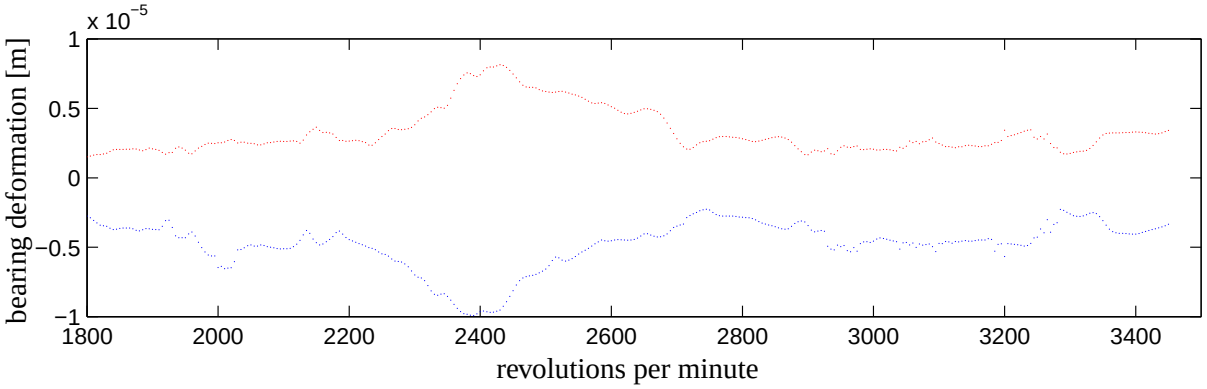

Figure 8: Dependence of extremes of roller-element bearing deformation on shaft's revolution for $\delta_{1,j} = \delta_1 + \pi/2$ (transversal radial direction)

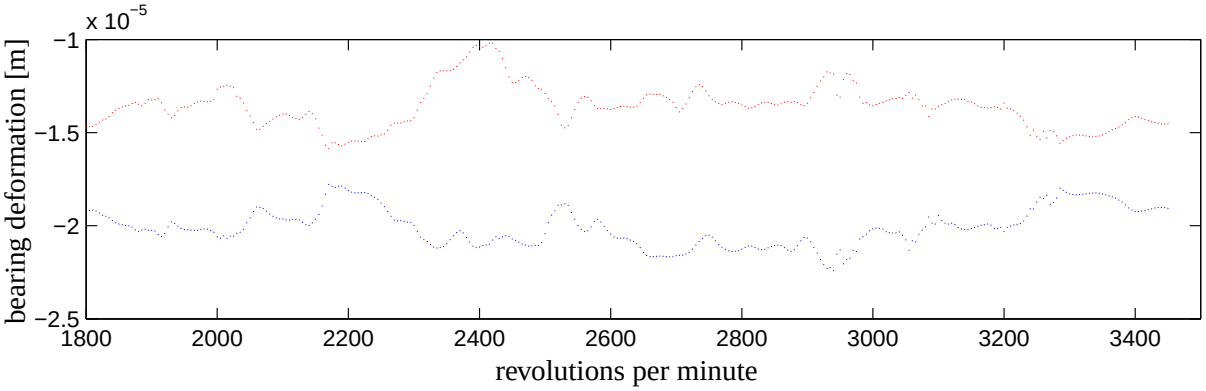

Figure 9: Dependence of extremes of roller-element bearing deformation on shaft's revolution for $\delta_{1,j} = \delta_1 + \pi$ (main radial direction)

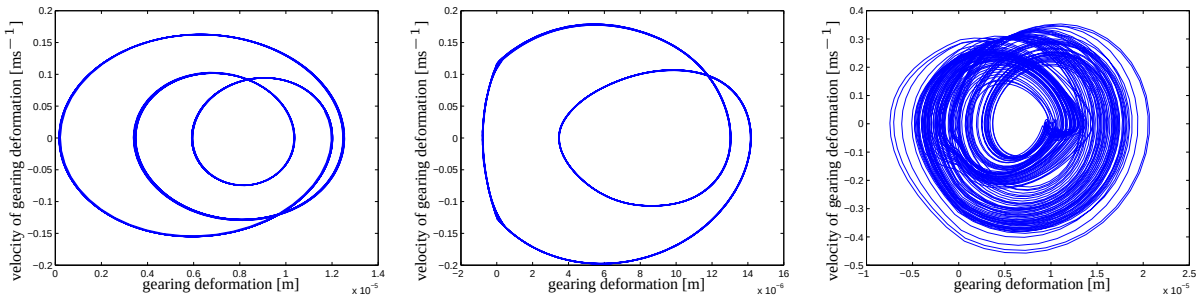

Figure 10: Phase trajectories of gearing deformation for $n = 2300$ rpm, $n = 2800$ rpm and $n = 3260$ rpm

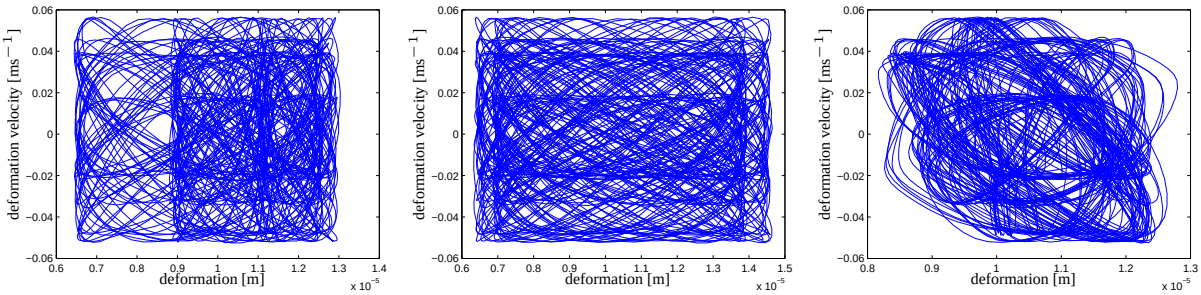

Figure 11: Phase trajectories of rolling-element deformation of the bearing B_1 in main radial direction for $n = 2300$ rpm, $n = 2800$ rpm and $n = 3260$ rpm

interruption. Fig. 11 shows phase trajectories of main radial ball-element deformation of the bearing B_1 for the three above defined states. It is interesting, the bearing element deformations have chaotic structure without any respect to the character of gearing deformation and journal centre motion. Further, it is astonishing, the phase trajectory of bearing element is enclosed in a rectangle and has rectangular structure.

The character of motion of bearing journal centre corresponds to the motion character of gearing, as fig. 12 displays.

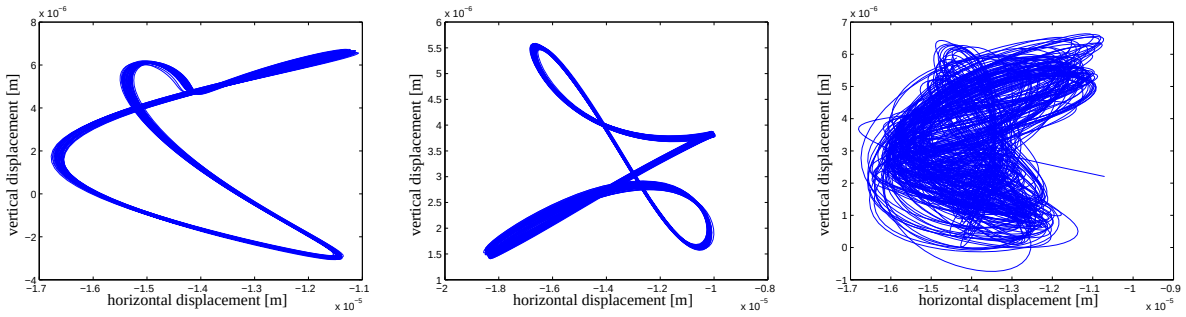

Figure 12: Orbits of journal centre of the bearing B_1 for $n = 2300$ rpm, $n = 2800$ rpm and $n = 3260$ rpm

5. Conclusion

The paper describes the methodology of the large coupled rotating systems modelling and the analysis of their nonlinear vibrations. The models of these systems suppose a flexible stator and nonlinear gear couplings between rotor subsystems and nonlinear rolling-element bearings. To model the couplings between rotor and stator subsystems the complex bearing model respecting real number of contact forces acting between journals and stator is used. The whole system model is created by means of the modal synthesis method which allows to rapidly reduce number of degrees of freedom of the mathematical model. The methodology is applied to the test-gearbox nonlinear vibrations excited by kinematic transmission error. The system response is computed using direct-time integration method and can be further used as a input for noise radiation analysis, see Hajžman and Byrtus (2006).

6. Acknowledgment

This work was supported by the research project MSM 4977751303 of the Ministry of Education, Youth and Sports of the Czech Republic.

7. References

Byrtus, M. & Zeman, V. (2005) Modelling and analysis of gear drive nonlinear vibration. *Proceedings of the Fifth EUROMECH Nonlinear Dynamics Conference.*

Hajžman, M. & Byrtus, M. (2006) Noise radiation of large rotating systems with nonlinear gear couplings. *Proceedings of the* 8^{th} *International scientific conference Applied mechanics.*

Krämer, E. (1993) Dynamics of Rotors and foundations. Springer-Verlag. Berlin.

Zeman, V. & Hajžman, M. (2005) Modelling of shaft system vibration with gears and rolling-element bearings. *Proceedings, Colloquium Dynamics of Machines 2005*.

Zeman, V. & Hlaváč, Z. (1995) Mathematical modelling of vibration of gear transmissions by modal synthesis method. *Proceedings of the Ninth World Congress on the Theory of Machines and Mechanisms*, Vol. 1, pp 397-400, Politechnico di Milano, Italy.